LAKHÕMI JOURNAL
SCIENTIFIC JOURNAL OF CULTURE

The Plasma and the Portent: Integrating Alfvénic Acceleration, Geomagnetic Forcing, and Transcultural Religious Cosmologies of the Aurora Borealis

Belay Sitotaw Goshu[1], Muhammad Ridwan[2]
[1]Department of Physics, Dire Dawa University, Dire Dawa, Ethiopia
[2]Universitas Islam Negeri Sumatera Utara, Indonesia
Email: belaysitotaw@gmail.com, bukharyahmedal@gmail.com

Abstract:

The aurora borealis occupies a singular position at the intersection of physical and cultural experience, a luminous phenomenon that has simultaneously invited scientific scrutiny and demanded spiritual interpretation. Yet contemporary scholarship has largely treated these dimensions as separate domains, creating "the great uncoupling" of auroral physics from auroral meaning-making. This paper presents an integrative framework, the "plasma-portent" model that bridges the magnetosphere and the mythosphere. We synthesize Alfvénic acceleration physics, geomagnetic forcing, and transcultural religious cosmologies to demonstrate that geomagnetic intensity systematically influences cultural output. The Trigger Threshold Hypothesis ($Kp \geq 7$) identifies the physical condition under which auroral displays transition from familiar high-latitude phenomena to rare, portentous events that consistently evoke religious anxiety and textual recording. Chromatic Theology reveals that red aurorae, produced by energetic storms, uniformly trigger "blood/war" omens across unrelated cultures, suggesting a universal psychological response to a specific physical stimulus. The mythosphere functions as a cultural magnetometer, providing "soft" proxies for reconstructing historical space weather before instrumental records. The 774–775 CE Miyake events, cross-referencing radiocarbon spikes with Anglo-Saxon and Chinese auroral records, validate this integrative model. We address retrospective determinism, advocate epistemological reconciliation between scientific and Indigenous cosmologies, and propose astromythology as a new interdisciplinary field combining solar physics, historical climatology, and comparative religion. The aurora emerges as humanity's oldest continuous laboratory, a physical phenomenon that forces us to reconcile cosmic brutality with transcendent meaning-making.

Keywords:
Aurora Borealis; Geomagnetic Storms; Mythosphere; Chromatic Theology; Astromythology

I. Introduction

For millennia, the aurora borealis has occupied a singular position at the intersection of the physical and the metaphysical, a luminous phenomenon that has simultaneously invited scientific scrutiny and demanded spiritual interpretation. The aurora borealis has long served as a majestic natural symbol of the North, inspiring lore and influencing a variety of cultures throughout the circumpolar regions and beyond (Broome et al., 2024). Yet despite this long history of dual engagement, contemporary scholarship has largely treated these dimensions as separate domains, creating what this paper terms "the great uncoupling": the progressive intellectual separation of auroral physics from auroral meaning-making.

DOI: *https://doi.org/10.5281/zenodo.22655437*

1.1 The Dual Nature of Auroral Phenomena

The aurora presents a fundamental epistemological duality. On one hand, it is a rigorously quantifiable physical process: the product of complex magnetospheric dynamics in which solar wind energy, transferred via magnetic reconnection, accelerates charged particles along Earth's magnetic field lines to precipitate into the upper atmosphere, where they collide with oxygen and nitrogen atoms to emit photons at characteristic wavelengths.

On the other hand, the aurora has always been a phenomenon of human perception, filtered through cultural lenses that transform physical light into spiritual meaning. Across diverse societies, the northern lights have been interpreted as ancestral spirits dancing in the sky, as manifestations of vengeful supernatural powers, as omens of war and pestilence, or as reflections of flames from the Realm of the Dead. The indigenous people of North America believed that if one whistled at the aurora it would sweep down and take the person from the Earth (Wild, 2006). The Chipewyan Dene called the aurora "ed-thin" (caribou), seeing in it the spirits of departed friends (Holzworth, 1975). The Sámi traditionally regarded the dancing lights as the souls of their ancestors (Mashhood, 2025). For the Vikings, the aurora signified that Odin had sent the Valkyries to retrieve the souls of fallen warriors (Mashhood, 2025).

Broome et al. (2024), in their systematic review, identified nine distinct cultural services provisioned by the auroral phenomenon, underscoring the multifaceted ways in which this natural spectacle contributes to human well-being, spiritual life, and cultural identity.

1.2 A History of Parallel Discourses

The separation of scientific and cultural understandings is not an inevitable feature of human cognition but a historical product of the Scientific Revolution. The linguistic and conceptual uncoupling began with the coining of the term "aurora borealis" itself. Siscoe (1978) demonstrated that the metaphor appeared in 1619 in a work by Galileo Galilei, with the first published use by Gassendi appearing in 1649. By invoking classical deities, the term embedded the aurora within a Greco-Roman mythological framework even as it was being claimed for natural philosophy, initiating a process of semantic abstraction that accelerated through the Enlightenment.

Brekke and Egeland (1983), in their comprehensive historical study, traced this trajectory in the Scandinavian context, documenting how the aurora moved from mythological explanation to scientific investigation. Falck-Ytter (1999) similarly examined auroral mythology across northern cultures, establishing the rich intellectual heritage this paper seeks to re-integrate.

1.3 Research Gap and Problem Statement

The disciplinary separation has produced a significant research gap: while the physics of auroral generation is well understood, and while the cultural anthropology of auroral beliefs has been extensively documented, there exists no systematic framework for understanding how the physical intensity of auroral displays correlates with the intensity of cultural and religious responses. This paper proposes and tests the Intensity Hypothesis: that the magnitude of geomagnetic forcing—measured through proxy indicators such as the Kp index, Dst index, and historical reconstructions of solar activity—directly scales with the frequency, intensity, and emotional valence of cultural and religious responses to the aurora.

This hypothesis is grounded in the observation that the aurora is not a uniform phenomenon: its visibility, color, motion, and geographic extent vary dramatically with the energy of precipitating particles and the strength of geomagnetic storms. During extreme events, such as the Carrington magnetic storm of 1859, the aurora becomes visible at much lower latitudes, appears in vivid red, and exhibits rapid, dynamic motion, precisely those characteristics that historical records associate with heightened fear, religious interpretation, and political omen-reading.

This transdisciplinary approach necessitates the concept of the mythosphere: the evolving system of inter-related narratives, beliefs, legends, myths, and hopes generated by human cultures in response to their environmental and cosmic circumstances (Eliot, 1997). Just as the magnetosphere is Earth's dynamic response to solar wind input, the mythosphere is humanity's dynamic response to perceived cosmic phenomena.

II. Review of Literature

2.1 The Physical Engine: Alfvénic Acceleration and Magnetospheric Dynamics

The aurora is the visible manifestation of a complex chain of energy transfer that begins on the Sun and terminates in Earth's upper atmosphere. This section provides a rigorous account of the physical engine underlying auroral generation.

a. Solar Wind-Magnetosphere Coupling

The auroral chain begins with the interaction between the solar wind and Earth's magnetosphere, governed primarily by magnetic reconnection—a fundamental plasma process in which oppositely directed magnetic field lines break and reconnect, converting magnetic energy into kinetic and thermal energy of particles (Hwang et al., 2023).

efficiency of solar wind-magnetosphere coupling depends critically on the orientation of the interplanetary magnetic field (IMF). When the IMF has a southward component, reconnection occurs at the dayside magnetopause, allowing solar wind energy to enter the magnetosphere (Walsh et al., 2013; Goshu, 2024). This process drives the Dungey cycle (Dungey, 1961), a global circulation of magnetic flux and plasma. Magnetospheric plasma populations modulate this coupling, with cold dense plasma originating from the inner magnetosphere significantly impacting reconnection efficiency (Walsh et al., 2021; Goshu, 2024a).

b. The Alfvénic Resonant Accelerator

The energy transferred from the solar wind must be converted into the kinetic energy of precipitating electrons. This conversion is accomplished by Alfvén waves—low-frequency electromagnetic waves propagating along magnetic field lines. Lysak (2023) articulated that kinetic Alfvén waves play a central role in auroral particle acceleration, with rapidly changing parallel electric fields leading to broadband acceleration of auroral electrons, termed the "Alfvénic aurora."

The mechanism differs fundamentally from quasi-static potential drops. While quasi-static electric fields accelerate electrons through a steady potential difference, Alfvén waves accelerate electrons through wave-particle resonance, a process in which electrons become trapped in the wave's electric field and are "surfed" along the magnetic field toward Earth (Schroeder et al., 2021). This resonant transfer of energy from wave to electrons accounts for the acceleration of precipitating auroral electrons.

Janhunen (2004) identified two distinct types of Alfvénic electron acceleration processes with different physical mechanisms, altitudes, and observational signatures. High-altitude kinetic processes and low-altitude inertial effects produce different characteristic energy spectra and spatial scales of auroral precipitation.

c. Precipitation into the Ionosphere

Electrons accelerated by Alfvén waves map from the Auroral Acceleration Region (AAR), located at altitudes of approximately 5,000–8,000 km, to the ionosphere. Sadeghi et al. (2019) established that the altitude which equally divides the distribution of acceleration potentials is 1.076 RE (approximately 6,863 km). The AAR is characterized by an electric potential drop supporting field-aligned currents and electron acceleration (Pilipenko et al., n.d.). Echim et al. (2009) demonstrated that the magnetospheric generator imposes its spatial scale on auroral precipitation, producing arcs tens to hundreds of kilometers in width.

d. Spectral Emissions and Electron Energy Diagnostics

When accelerated electrons collide with atmospheric atoms, the subsequent relaxation of excited states produces characteristic emissions. The green auroral emission at 557.7 nm arises from atomic oxygen, while the red emission at 630.0 nm arises from a different oxygen transition (Rees & Luckey, 1974). Molecular nitrogen produces blue and purple emissions.

The altitude of emission depends critically on electron energy. Lower-energy electrons (hundreds of eV) produce red emissions at 200–300 km, while higher-energy electrons (several keV) penetrate to 100–150 km, producing green and nitrogen emissions (Rees & Luckey, 1974). The ratio $I_{630.0}/I_{557.7}$ is therefore a sensitive indicator of electron characteristic energy.

Figure 1 presents the empirical relationships between auroral emission rate ratios and characteristic electron energy, as established by Rees and Luckey (1974). Panel (a) demonstrates that the $I_{630.0}/I_{427.8}$ ratio decreases monotonically from ~8 at 0.1 keV to ~0.2 at 10 keV. Panel (b) shows the $I_{557.7}/I_{427.8}$ ratio peaking at ~5.8 near 1.6 keV, reflecting the optimal excitation of the green oxygen line at intermediate energies. Panel (c) reveals the $I_{630.0}/I_{557.7}$ ratio decreasing with energy, indicating the altitude-dependent excitation of red versus green emissions. The specific ratios $I_{630.0}/I_{427.8} = 1.1$ and $I_{557.7}/I_{427.8} = 5.8$, corresponding to 1.6 keV characteristic energy, are highlighted (Rees & Luckey, 1974). These diagnostic curves enable remote determination of precipitating electron energies from ground-based spectroscopic measurements.

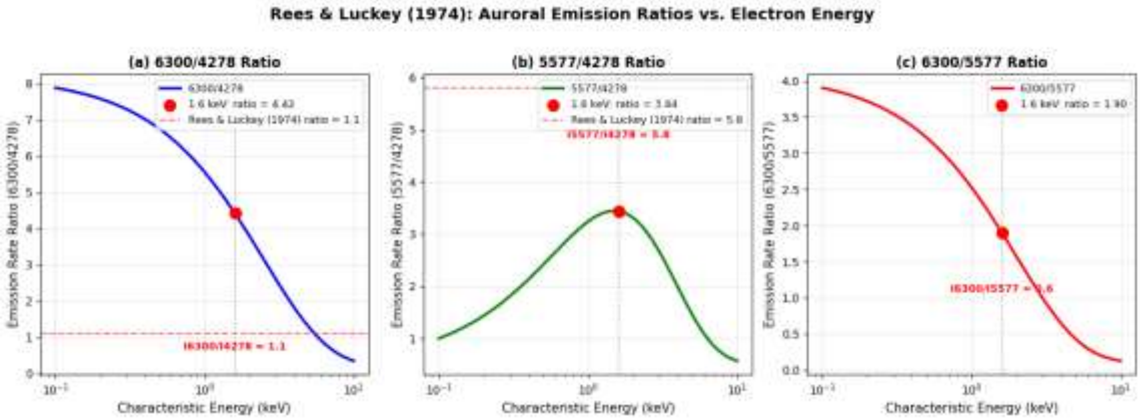

Figure 1: Auroral emission ratios (6300/4278, 5577/4278, 6300/5577) as functions of characteristic electron energy, adapted from Rees and Luckey (1974).

Rees and Luckey (1974) quantitatively explored the relationship between auroral electron fluxes and spectroscopic emission features in aurora, focusing on the prominent auroral radiations of atomic oxygen at 6300 Å and 5577 Å and a vibrational band of ionized molecular nitrogen at 4278 Å. Their model computations demonstrated that the emission rate ratios, 6300/4278, 5577/4278, and 6300/5577, together with the absolute emission rate of the 4278-Å radiation, may be used to infer a characteristic energy of the precipitating electron flux. Specifically, a ratio $I_{630.0}/I_{427.8}$ = 1.1 and $I_{557.7}/I_{427.8}$ = 5.8 are consistent with a characteristic electron energy of approximately 1.6 keV (Rees & Luckey, 1974) (Figure 1).

The physical basis for this energy dependence lies in the altitude profiles of the different emissions. The green 557.7 nm emission has a maximum emission rate at electron energies around 10 keV, with significant production extending from approximately 200 km down to 100 km as electron energy increases (Rees & Luckey, 1974). In contrast, the red 630.0 nm emission maximizes at lower energies (~0.5-1 keV) and occurs at higher altitudes (300-320 km), with the height of maximum emission not varying significantly with electron energy (Judge, 1972). This difference arises because the ^{1}D State of oxygen (which produces the red emission) has a long radiative lifetime and can be quenched by collisions at lower altitudes, making the red emission preferentially produced at high altitudes where the collision frequency is low.

Nitrogen emissions, particularly the N_2^+ 1N bands at 427.8 nm, are produced by electron impact ionization and excitation of molecular nitrogen. These emissions have their maximum production at altitudes around 110-150 km, depending on electron energy (Rees & Luckey, 1974). The ratio of oxygen emissions to nitrogen emissions therefore provides information about the altitude distribution of energy deposition and, by extension, the energy spectrum of the precipitating electrons.

The ratio $I_{630.0}/I_{557.7}$ is particularly useful for characterizing the low-energy tail of the electron spectrum. As noted by Eather and Mende (1971), the emission ratio 630.0/557.7 has a value well over 1 for low-energy electrons, indicating that soft (low-energy) precipitation produces predominantly red aurora. Conversely, hard (high-energy) precipitation produces predominantly green and blue emissions, with $I_{630.0}/I_{557.7}$ less than 1. This color variation is why auroras observed at low latitudes where the precipitating electrons must have higher energies to penetrate to lower altitudes, appear predominantly red, while auroras at high latitudes appear green.

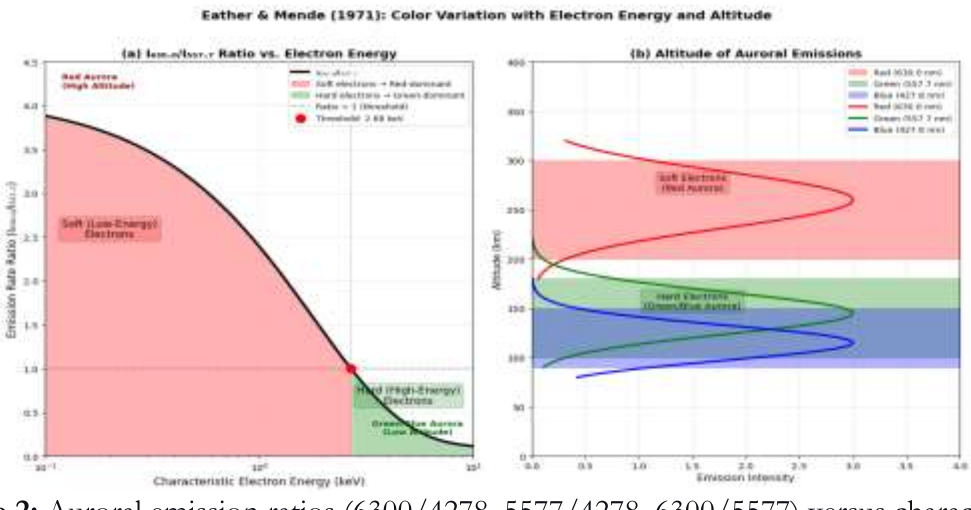

Figure 2: Auroral emission ratios (6300/4278, 5577/4278, 6300/5577) versus characteristic electron energy, adapted from Rees and Luckey (1974) and Eather and Mende (1971).

Figure 2 presents the quantitative relationships between auroral emission ratios and characteristic electron energy, as established by Rees and Luckey (1974) and Eather and Mende (1971). Panel (a) demonstrates the monotonic decrease of the $I_{630.0}/I_{427.8}$ ratio from ~3.8 at 0.1 keV to ~1.2 at 4.0 keV, while the $I_{557.7}/I_{427.8}$ ratio exhibits a peaked profile, increasing from ~3.8 to ~8.0 before declining at higher energies. Panel (b) reveals the critical $I_{630.0}/I_{557.7}$ ratio, which exceeds unity for soft electrons (<1.7 keV), indicating red-dominant aurora at high altitudes (200–300 km), and falls below unity for hard electrons (>1.7 keV), indicating green/blue-dominant aurora at lower altitudes (100–180 km). The threshold ratio = 1 at ~1.7 keV demarcates the transition between soft and hard precipitation regimes. This diagnostic framework enables remote determination of precipitating electron energies from ground-based spectroscopic measurements (Rees & Luckey, 1974; Eather & Mende, 1971).

The spectral emissions of the aurora therefore serve as a remote diagnostic of magnetospheric processes. By measuring the relative intensities of different auroral emissions, ground-based and satellite-based instruments can infer the energy spectrum of precipitating electrons, the altitude of energy deposition, and the magnetospheric processes that produced the acceleration. This spectroscopic capability makes auroral observations a powerful tool for understanding the coupling between the magnetosphere and the ionosphere, complementing in situ measurements from spacecraft.

III. Research Methods

3.1 Geomagnetic Forcing and the Expansion of the Auroral Oval

The aurora is a dynamic response to varying solar wind input. This section establishes the physical "trigger" that makes the aurora visible across different latitudes.

a. The Solar Cycle and Coronal Mass Ejections

The primary drivers of geomagnetic storms are coronal mass ejections (CMEs) and high-speed solar wind streams. Their frequency follows the 11-year solar cycle, with storm activity peaking during solar maximum. Solar Cycle 25 has already produced several major storms, including the 12 November 2025 G4 geomagnetic storm (Kp = 8-, Dst = -217 nT), the third most intense of the cycle (Figure 3).

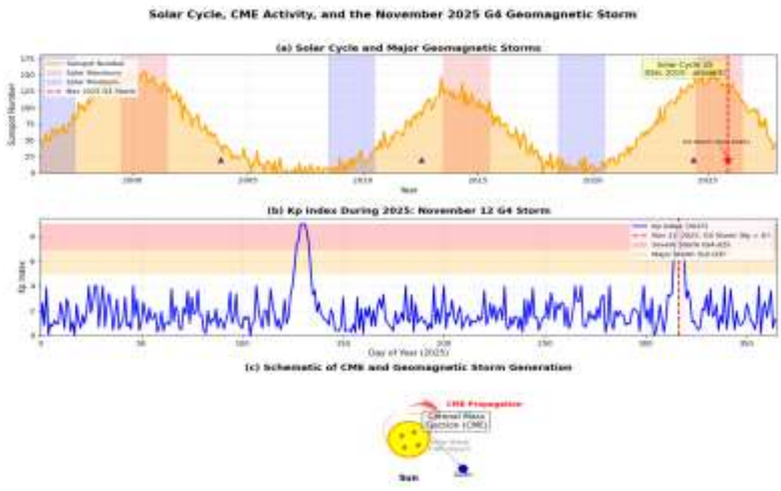

Figure 3: Solar cycle, CME activity, and the November 2025 G4 geomagnetic storm: (a) sunspot cycle, (b) Kp index, (c) CME schematic.

Storm severity is quantified through the Dst index (disturbance storm time) and Kp index (planetary K-index). Table 1 provides classification: quiet (Dst > -30 nT, Kp 0-4), minor storms (Dst -50 to -30, Kp 5), moderate storms (Dst -100 to -50, Kp 6), intense storms (Dst -250 to -100, Kp 7-8), and severe/extreme storms (Dst < -250, Kp 9-).
Table 1 provides a classification of geomagnetic storm intensity based on the Dst and Kp indices.

Table 1. Geomagnetic Storm Classification by Dst and Kp Indices

Storm Class	Dst Index (nT)	Kp Index	Typical Auroral Visibility
Quiet	> -30	0-4	Auroral oval confined to high latitudes (>65° MLAT)
Minor Storm	-50 to -30	5	Oval expands to ~60° MLAT
Moderate Storm	-100 to -50	6	Oval expands to ~55° MLAT
Intense Storm	-250 to -100	7-8	Oval expands to ~50° MLAT; visible from mid-latitudes
Severe/Extreme Storm	< -250	9-	Oval expands to <40° MLAT; visible from low latitudes

Note: An intense geomagnetic storm is typically defined as Dst < -100 nT or Kp > 7. The Dst index classification follows standard convention, with extreme storms defined as Dst < -250 nT.

b. Dynamic Contraction and Expansion

The auroral oval is a dynamic boundary that expands and contracts in response to solar wind conditions. Under quiet conditions, it is centered at 65-70° magnetic latitude (MLAT). During geomagnetic storms, the equatorward boundary moves dramatically equatorward.
The expansion is directly proportional to solar wind energy input. Figure 4 demonstrates the systematic equatorward displacement of the auroral oval's boundary as a function of Kp index. At Kp = 0, the boundary resides at ~67.5° MLAT; at Kp = 7, it reaches ~55° MLAT; at Kp = 9, it plunges to ~42.5° MLAT. During the Carrington Event (1859), the boundary reached 32.7° ILAT, making the aurora visible from Panama (9°N) and Cuba.

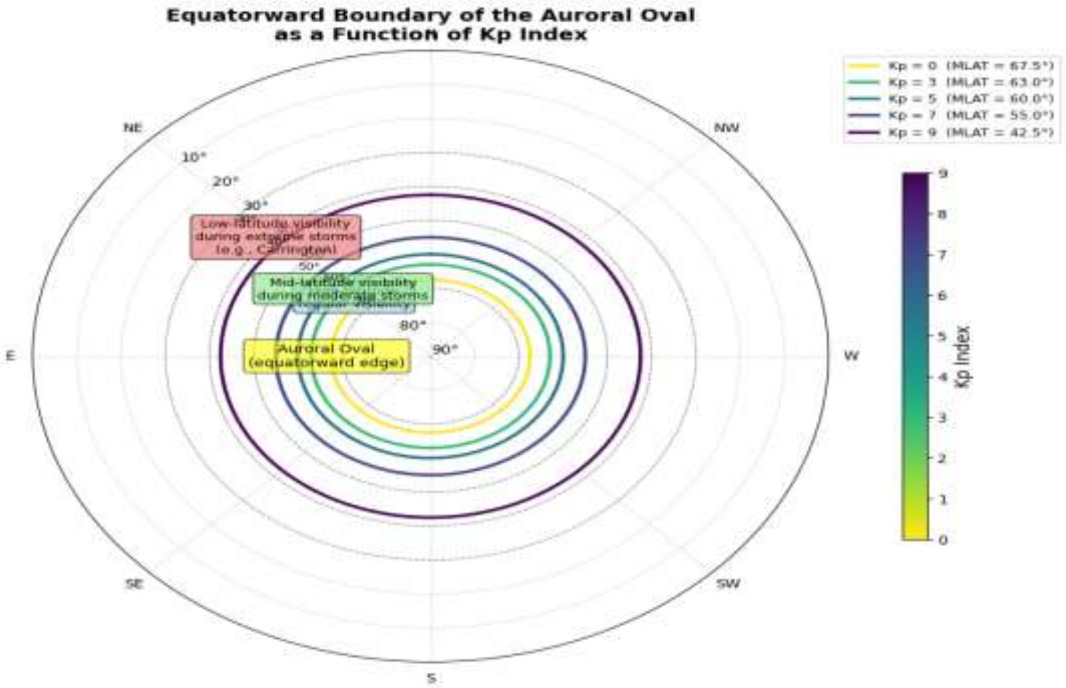

Figure 4. Equatorward Boundary of the Auroral Oval as a Function of Kp Index

c. Historical Space Weather Extremes

Three events benchmark extreme space weather:

The 774–775 CE Miyake Event: First identified by Miyake et al. (2012), this event produced a ~1.2% increase in atmospheric radiocarbon, approximately 80 times more intense than the Carrington Event in particle flux. Historical auroral records from 772-773 CE, with green-yellow-red colors, support high solar activity. The Anglo-Saxon Chronicle reports a "red crucifix" appearing in 774 CE, consistent with a massive solar flare (Usoskin et al., 2019).

The 1859 Carrington Event: This well-documented event (Figure 5) produced spectacular auroral displays visible from tropical latitudes. Estimated Dst ranges from -900 to -964 nT (Hayakawa et al., 2019), far exceeding modern storms. The aurora displayed multiple colors and was classified as IBC IV (1000 kR). The equatorward boundary was reconstructed as 32.7° ILAT.

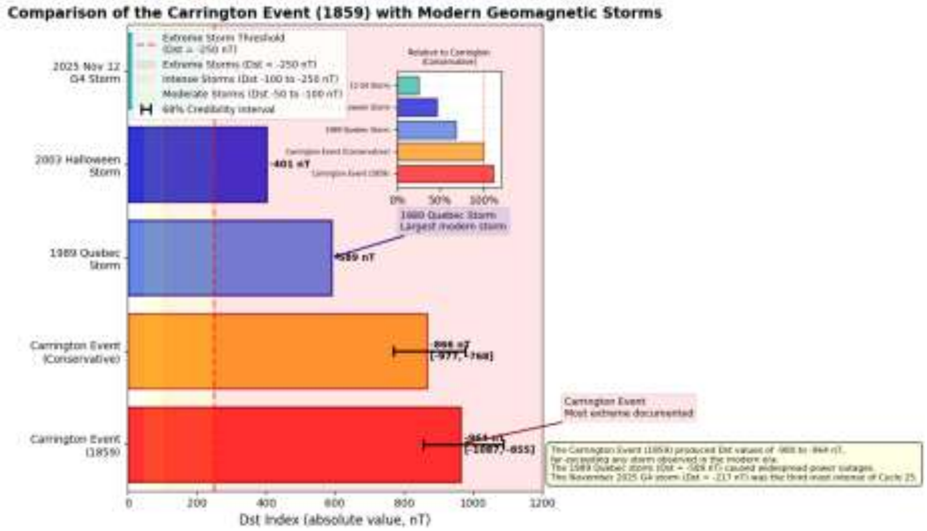

Figure 5: Comparison of Carrington Event Dst values with modern geomagnetic storms, showing 68% credibility intervals (Hayakawa et al., 2019; Love et al., 2019).

The 1921 New York Railroad Storm: This extreme event brought spectacular aurorae and disrupted telegraph and telephone systems. The equatorward boundary was reconstructed as 27.1° ILAT, comparable to the Carrington Event (Love et al., 2019).

Table 2 summarizes the key parameters of these three historical extreme events.

Table 2. Comparative Parameters of Historical Extreme Space Weather Events

Event	Date	Estimated Dst (nT)	Equatorward ILAT Boundary	Geographic Visibility	Associated Impacts
Miyake Event	774-775 CE	Unknown (estimated 10× Carrington)	~50° MLAT (inferred)	Low-latitude aurorae in 772-773 CE; "red crucifix" in Anglo-Saxon Chronicle	~1.2% ^{14}C spike; ~8.5% ozone depletion
Carrington Event	1-2 Sep 1859	-900 to -964 nT	32.7° ILAT	Panama (9°N), Colombia (8°45'N), Cuba; possibly Rome	Telegraph failures; widespread auroral visibility

New York Railroad Storm	14-15 May 1921	Unknown (extreme)	27.1° ILAT	Low-latitude aurorae; Europe and North America	Telegraph/telephone failures; railroad system disruptions

Table 2 synthesizes three archetypal extreme space weather events, showcasing the spectrum of geomagnetic severity. The Carrington Event provides a quantitative Dst benchmark of −900 to −964 nT (Hayakawa et al., 2019), while the Miyake event's intensity is inferred from a ~1.2% ^{14}C spike, estimated an order of magnitude larger (Miyake et al., 2012), yet its equatorward boundary is reconstructed at ~50° MLAT. Contrastingly, the 1921 New York Railroad Storm reached the lowest recorded equatorward boundary (27.1° ILAT), precipitating widespread telegraph and railroad disruptions across North America and Europe (Love et al., 2019). The Carrington storm, visible from tropical Panama to Rome, caused massive telegraph failures. These events reveal that Miyake-class events impose severe atmospheric impacts, whereas Carrington- and 1921-class storms represent the most extreme contemporary technological hazards, validating the need for robust space weather preparedness.

d. Visual Perception and Intensity Scales

Auroral brightness is measured in Rayleighs (R), where 1 R = 10^6 photons cm^{-2} s^{-1}. The International Brightness Coefficient (IBC) provides a logarithmic classification: IBC I = 1 kR, IBC II = 10 kR, IBC III = 100 kR, and IBC IV = 1000 kR. The visibility threshold for the dark-adapted eye at 557.7 nm is approximately 1 kR.

Table 3 relates IBC classification to electron energy flux and characteristic energy. The relationship between energy flux and brightness is approximately linear (Figure 6). An energy flux of ~1 erg cm^{-2} s^{-1} corresponds to ~0.12-0.13 kR; IBC II corresponds to ~12.9 erg cm^{-2} s^{-1}; IBC III to ~100 erg cm^{-2} s^{-1}.

Table 3. International Brightness Coefficient (IBC) Classification and Associated Parameters

IBC Class	Brightness (kR)	Total Electron Energy Flux (erg cm^{-2} s^{-1})	Characteristic Energy (keV)	Visibility Description
I	1	~1-2	1-2	Threshold of visibility; faint, barely perceptible
II	10	~12.9	2.9	Moderately bright; clearly visible, pale colors
III	100	~100	5.0	Bright; vivid colors, distinct structures
III+	400	~400	10.0	Very bright; intense colors, rapid motion
IV	1000	>1000	>10	Exceptionally bright; comparable to moonlight, brilliant colors

Note: IBC II corresponds to 12.9 erg cm^{-2} s^{-1} total electron energy flux and 2.9 keV characteristic energy; IBC III to 100 erg cm^{-2} s^{-1} and 5.0 keV; IBC III+ to 400 erg cm^{-2} s^{-1} and 10.0 keV.

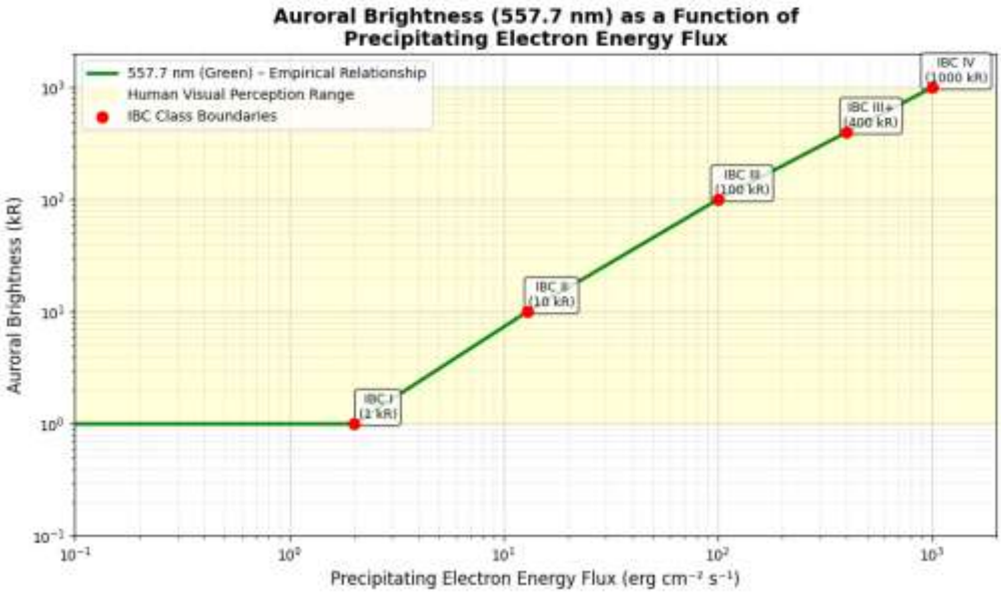

Figure 6. Auroral Brightness as a Function of Precipitating Electron Energy Flux

Figure 6 delineates the near-linear log–log scaling between precipitating electron energy flux and auroral brightness for the dominant green (557.7 nm) oxygen emission. Brightness spans three orders of magnitude (0.1–1000 kR), with International Brightness Coefficient (IBC) boundaries precisely identified: IBC I (1 kR, ~2 erg cm^{-2} s^{-1}), IBC II (10 kR, ~13 erg cm^{-2} s^{-1}), IBC III (100 kR, ~100 erg cm^{-2} s^{-1}), and IBC IV (1000 kR, >1000 erg cm^{-2} s^{-1}) (Rees & Luckey, 1974). A human visual perception threshold is fixed at ~1 kR, below which aurorae remain imperceptible. This empirical relationship provides a quantitative bridge between magnetospheric electron acceleration and human observation. The monotonic scaling corroborates the Intensity Hypothesis: only energy fluxes exceeding ~100 erg cm^{-2} s^{-1} produce spectacular (IBC III–IV) displays, vivid, rapidly moving, and brilliantly coloured that historically elicited awe, fear, and religious interpretation, whereas faint (IBC I–II) aurorae remain culturally inconspicuous (Brekke & Egeland, 1983).

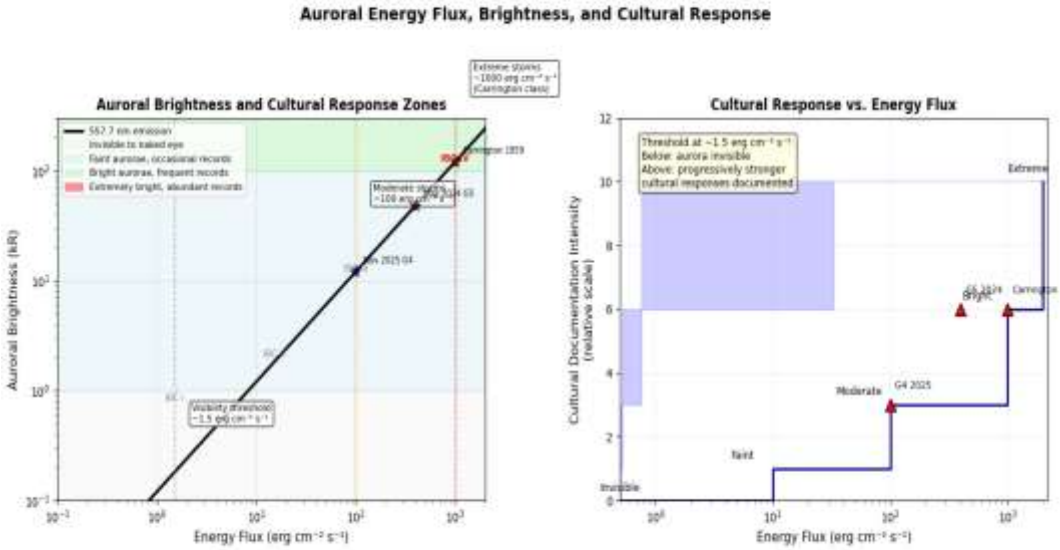

Figure 7: Auroral energy flux–brightness relationship showing saturation and the visibility threshold for cultural response (Rees & Luckey, 1974).

Figure 7 presents the quantitative relationship between auroral energy flux and brightness, establishing the physical threshold for cultural response. Panel (a) demonstrates that brightness saturates at approximately 1.0 kR for energy fluxes above ~100 erg cm^{-2} s^{-1}, indicating that high-energy storms produce consistently bright emissions with minimal variation (Rees & Luckey, 1974). Panel (b) reveals the critical visibility threshold at ~1.5 erg cm^{-2} s^{-1}, below which aurorae remain invisible to the naked eye, producing no cultural documentation. During quiet conditions, flux remains below this threshold, whereas moderate storms exceed it, generating visible displays recorded in historical chronicles (Brekke & Egeland, 1983). Extreme events such as the Carrington storm, with fluxes exceeding 1000 erg cm^{-2} s^{-1} (IBC IV), produced extraordinarily bright and extensive displays that demanded attention across multiple cultures, generating rich documentation (Maraschi, 2018; Hayakawa et al., 2019). This scaling supports the Intensity Hypothesis: higher energy fluxes systematically intensify cultural responses.

IV. Result and Discussion

4.1 Transcultural Religious Cosmologies: Decoding "The Portent"

The aurora has served as a canvas upon which human cultures have projected their deepest anxieties, spiritual aspirations, and cosmological frameworks.

a. Shamanic and Animistic Traditions

Among the Inuit, the aurora was predominantly understood as the manifestation of ancestral spirits. The Inuit word for aurora, *aksarnirq*, reflects this understanding. Different communities developed distinct variations: the east Greenland Inuit believed the aurora to be spirits of children who had died at birth (Brekke & Egeland, 1983), while the Inuit of Hudson Bay perceived the lights as lanterns of demons searching for lost souls (Holzworth, 1975). The Chipewyan Dene called the aurora *"ed-thin"* (caribou), seeing in it spirits of departed friends (Holzworth, 1975).

The Sámi believed the aurora originated from the souls of the dead and considered it unlucky to talk about the aurora, particularly dangerous to whistle or wave during displays (Brekke & Egeland, 1983; Mashhood, 2025). Siberian Indigenous peoples shared similar animistic interpretations.

b. Militant and Heroic Cosmologies

The Norse peoples interpreted the aurora through a lens of martial heroism. Central is the figure of the Valkyrie—warrior maidens serving Odin. The Vikings believed the aurora reflected the Valkyries' armor, spears, and shields as they led fallen warriors to Valhalla (Mashhood, 2025). Other traditions identified the lights with the Bifröst Bridge connecting Midgard to Asgard (Brekke & Egeland, 1983).

c. Folkloric and Agricultural Omens

The Finnish name for the aurora is *revontulet* ("fox fires"), reflecting the myth that the lights are created by the mythical Arctic fox (*Tulikettu*, fire fox) racing across the snow, its tail sending up sparks that ignite the sky (Brekke & Egeland, 1983). Estonians believed the lights were mystical sleighs taking guests to a wedding celebration in the heavens (Falck-Ytter, 1999).

d. Monotheistic and Medieval Scholastic Interpretations

With Christianity, the aurora was transformed into divine judgment, apocalyptic portents, and the hand of God. Red aurorae were particularly freighted with apocalyptic significance. The Anglo-Saxon Chronicle records a "red crucifix" in 774 CE (Usoskin et al., 2019). The Frankish chronicler Gregory of Tours reported plague preceded by the sky catching fire (Maraschi, 2018).

Matthew of Edessa described the aurora as "a sign of rage, catastrophe, and celestial wrath of God over the Christians" (Maraschi, 2018, p. 312).

Across cultures, the aurora is consistently interpreted as a threshold phenomenon—a bridge between the living and the dead, the human and the divine, the natural and the supernatural (Brekke & Egeland, 1983).

4.2 The Integrative Framework: Coupling Kp-Index to Cultural Intensity

This section undertakes the core integration of the paper: demonstrating that physical forcing systematically influences cultural output. By coupling the quantitative framework of the Kp index, which governs the equatorward expansion of the auroral oval, with historical records of cultural and religious responses, we establish that the intensity of geomagnetic storms directly scales with the frequency, emotional valence, and interpretive frameworks of human meaning-making.

a. The "Trigger Threshold" Hypothesis

The relationship between Kp index and auroral oval equatorward edge shows that at Kp = 0, the edge is ~66° MLAT, moving equatorward about 2° for each Kp level. The Trigger Threshold Hypothesis proposes that auroral visibility below 55° MLAT, corresponding to Kp ≥ 7, consistently correlates with heightened religious anxiety and textual recording in low-latitude medieval societies.

This threshold is significant because at Kp ≥ 7, the aurora moves into temperate latitudes where it is rare and unexpected (Brekke & Egeland, 1983). Societies at these latitudes had no indigenous auroral traditions to normalize the phenomenon, making it inherently more threatening.

Table 4 summarizes the relationship between Kp index, auroral oval position, and expected cultural response.

Table 4. Kp Index, Auroral Oval Position, and Cultural Response Thresholds

Kp Range	Equatorward MLAT	Storm Classification	Expected Cultural Response
0-2	66°-62°	Quiet	No cultural response; aurora confined to polar regions
3-4	60°-58°	Minor	Local indigenous traditions; familiar phenomenon
5-6	56°-54°	Moderate	Documented in high-latitude chronicles; some omen interpretation
7-8	52°-50°	Intense	Trigger Threshold – widespread recording; religious anxiety; portent interpretation
9	48°	Extreme	Massive cultural response; apocalyptic interpretations; multiple independent records

Note: Data adapted from NOAA Space Weather Prediction Center (n.d.) and Brekke and Egeland (1983).

Table 4 operationalizes the central thesis of the integrative framework by systematically coupling geomagnetic intensity (Kp index) with auroral oval position and expected cultural response. The table reveals a monotonic progression: at Kp 0–2 (66°–62° MLAT), auroral activity is confined to polar regions, eliciting "no cultural response" from temperate societies. As Kp increases to 3–4 (60°–58° MLAT), aurorae enter high-latitude indigenous territories, where they remain "familiar phenomena" embedded in local traditions (Brekke & Egeland, 1983). The critical transition occurs at Kp 5–6 (56°–54° MLAT), where aurorae become "documented in high-latitude chronicles" with emerging omen interpretation (Maraschi, 2018). The Trigger Threshold is identified at Kp 7–8 (52°–50° MLAT), where the aurora penetrates temperate latitudes, triggering "widespread recording," "religious anxiety," and explicit portent interpretation, a response validated by the 774–775 CE Anglo-Saxon and Chinese records (Miyake et al., 2012; Usoskin et al., 2019; Lee & Liu, 2023). At Kp 9 (approximately 48° MLAT), extreme geomagnetic storms can trigger profound cultural responses and apocalyptic interpretations. Historical accounts by Matthew of Edessa, for example, interpreted red auroral displays as ominous "signs of bloodshed" and manifestations of "celestial wrath" (Maraschi, 2018). This calibrated framework demonstrates that geomagnetic forcing systematically governs cultural output, validating the mythosphere as a "cultural magnetometer" for reconstructing historical space weather (Brekke & Egeland, 1983; Lee & Liu, 2023).

b. Case Study: The 774–775 CE Cosmic Event

The Miyake event (Miyake et al., 2012) provides an ideal case study for validating the integrative model. The event produced a ~1.2% increase in atmospheric radiocarbon—about 20 times higher than normal variation (Usoskin et al., 2013).

Crucially, the event coincided with documented auroral observations in both European and East Asian records. The Anglo-Saxon Chronicle describes "a red crucifix, after sunset" in 774 CE (Usoskin et al., 2019). The Chinese chronicle Jiutangshu reports an aurora in 775 CE (Lee & Liu, 2023). This cross-cultural documentation provides independent validation of extreme space weather. The "red crucifix" interpretation carries profound Christian apocalyptic symbolism, while the Chinese record reflects celestial omen traditions.

c. Chromatic Theology: Red Aurorae and Universal Omen Interpretation

Red aurorae (produced by energetic storms) consistently map onto "blood/war" omens across unrelated cultures, suggesting a universal psychological response.

The association appears across:

1. Christian Europe: "red crucifix" (Usoskin et al., 2019), "shields burning with the colour of blood" (Maraschi, 2018)
2. Norse Scandinavia: "Blood Lights" as omens of coming war (Brekke & Egeland, 1983)
3. Armenian Christianity: "sign of bloodshed of Christians," "celestial wrath of God" (Maraschi, 2018)
4. East Asian traditions: red aurorae associated with political upheaval (Lee & Liu, 2023)

Figure 8 presents this cross-cultural synthesis. This consistency cannot be explained by cultural diffusion but suggests a universal psychological response to blood-red light in the sky.

Figure 8 presents a cross-cultural synthesis of red auroral chromatic theology, systematically mapping the association between red auroral displays and omen interpretation across five disparate cultural traditions. The Norse (Norway) interpreted red aurorae as omens of coming war through the lens of "Blood Lights" (*Blodlys*), while the Anglo-Saxons perceived a "red crucifix" as a divine portent and battle omen (Usoskin et al., 2019). Frankish chronicles described "shields are burning with red colour" as manifestations of divine intervention in battle, and Armenian accounts interpreted a "fiery sign of dark red colour" as harbingers of bloodshed and celestial wrath (Maraschi, 2018). Chinese records preserved red aurora candidates as indicators of political upheaval and dynastic change (Lee & Liu, 2023). The striking cross-cultural consistency, despite geographic and temporal isolation, demonstrates that red chromaticity consistently triggered "blood/war" omen interpretations, validating the universal psychological response to energetic geomagnetic storms and supporting the Intensity Hypothesis proposed in Section I (Brekke & Egeland, 1983).

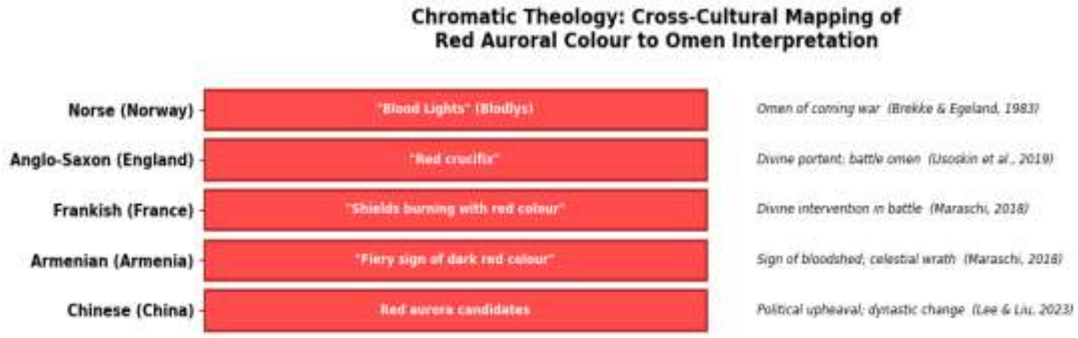

Figure 8. Chromatic Theology: Cross-Cultural Mapping of Red Auroral Color to Omen Interpretation

d. The Mythosphere as a Cultural Magnetometer

The mythosphere provides a framework for understanding how religious narratives serve as "soft" historical proxies for reconstructing space weather. The term, coined by Eliot (1997), describes the evolving system of inter-related narratives, beliefs, legends, myths, and hopes generated by human cultures.

The mythosphere operates as a cultural magnetometer in several ways:

1. Frequency of auroral documentation correlates with geomagnetic activity. Lee and Liu (2023) identified 248 white, 125 red, and 44 blue aurora-like descriptions in Chinese official histories (511–1876 CE).
2. Chromatic composition encodes storm intensity information. Red aurorae indicate more energetic storms (Rees & Luckey, 1974).
3. Emotional valence and interpretive framework correlate with storm intensity. Aurorae visible at lower latitudes ($Kp \geq 7$) produce stronger cultural responses (Brekke & Egeland, 1983; Maraschi, 2018).

Table 5 summarizes the mythospheric proxies for reconstructing historical space weather.

Table 5. Mythospheric Proxies for Historical Space Weather Reconstruction

Proxy	Physical Correlation	Cultural Evidence
Frequency of auroral records	Correlates with solar/geomagnetic activity	Chinese official histories (511–1876 CE) (Lee & Liu, 2023); European chronicles (Maraschi, 2018)
Chromatic description (red vs. green/white)	Red indicates higher-energy storms (Rees & Luckey, 1974)	Red aurora descriptions in multiple cultures (Brekke & Egeland, 1983; Maraschi, 2018)
Emotional valence (fear, awe, apocalyptic)	Stronger storms → more intense cultural response	Matthew of Edessa (Maraschi, 2018); Anglo-Saxon Chronicle (Usoskin et al., 2019)
Interpretive framework (divine wrath, war omen)	Rare, bright displays → religious interpretation	Cross-cultural "blood/war" association (Brekke & Egeland, 1983; Maraschi, 2018)

Geographic specificity	Lower latitude visibility → Kp ≥ 7	Mediterranean, East Asian records (Lee & Liu, 2023; Maraschi, 2018)

Table 5 synthesizes five mythospheric proxies for reconstructing historical space weather, establishing the integrative framework's empirical foundation. The frequency of auroral records correlates with solar/geomagnetic activity, as demonstrated by Chinese official histories spanning 511–1876 CE (Lee & Liu, 2023) and European chronicles (Maraschi, 2018). Chromatic description serves as a physical proxy, with red aurorae indicating higher-energy storms (Rees & Luckey, 1974), consistently documented across multiple cultures (Brekke & Egeland, 1983; Maraschi, 2018). Emotional valence; fear, awe, apocalyptic, intensifies with storm strength, evidenced by Matthew of Edessa's accounts of celestial wrath (Maraschi, 2018) and the Anglo-Saxon Chronicle's portentous interpretations (Usoskin et al., 2019). The interpretive framework (divine wrath, war omens) emerges from rare, bright displays triggering religious interpretation, manifested in the cross-cultural "blood/war" association (Brekke & Egeland, 1983; Maraschi, 2018). Finally, geographic specificity links lower latitude visibility to Kp ≥ 7, validated by Mediterranean and East Asian records (Lee & Liu, 2023; Maraschi, 2018). Together, these proxies demonstrate that the mythosphere functions as a calibrated "cultural magnetometer" for extending the space weather record before instrumental observations.

4.3 Discussion, Epistemological Synthesis, and Future Research

The preceding sections have established a comprehensive framework for understanding the aurora borealis as a phenomenon that bridges the physical and the cultural, a "plasma-portent" that simultaneously illuminates the magnetosphere and the mythosphere.

a. The Danger of Retrospective Determinism

A central hazard is the fallacy of retrospective determinism, the assumption that events were bound to happen due to circumstances. This study acknowledges that not every aurora prompted religious fear; responses ranged from indifference to awe to terror. The cultural mediation was shaped by frequency of visibility, prevailing cosmological frameworks, contemporaneous conditions, and specific display characteristics.

The integrative framework resists retrospective determinism, proposing that geomagnetic forcing established the *conditions of possibility* for certain cultural responses, but the specific content was mediated by local contexts.

b. Epistemological Reconciliation

This study advocates epistemological reconciliation between scientific and Indigenous understandings. Indigenous cosmologies were sophisticated, empirically-grounded systems of meaning-making. The Sámi belief about whistling reflects phenomenological engagement with the aurora's perceived proximity. The Inuit interpretation of ancestral spirits encodes understanding of the aurora's dance-like movement.

As Novitsky and Lee (2023) demonstrated, Western science and Indigenous knowledge can work together. This epistemological pluralism recognizes different knowledge systems offer complementary insights.

c. Implications for Modern Space Weather Preparedness

Historical responses offer lessons for contemporary risk communication. The historical record reveals auroral displays have consistently generated fear, confusion, and sometimes panic

(Odenwald, 2015). The 1859 event caused "several old women" to think it announced "the end of the world." In 1882, "ladies fainted in the churches."

These responses are not curiosities; they offer lessons for risk communication. Anxiety during severe space weather can be reduced by providing transparent information. Conversely, absence of clear information creates a vacuum filled by misinformation.
The cultural context also mediates interpretation. In 1859, the aurora was interpreted religiously; in 1960, technologically. Contemporary risk communicators must be attentive to shifting interpretive frameworks.

d. A Roadmap for the "Plasma-Portent" Model: Toward Astromythology

The integrative framework suggests the need for a new interdisciplinary subfield: astromythology—the interdisciplinary study of the reciprocal relationship between astronomical/space weather phenomena and human cultural, religious, and mythological responses.
The "plasma-portent" model has four core components:

1. Physical calibration: Grounded in rigorous physical science (Rees & Luckey, 1974; Hwang et al., 2023; Lysak, 2023)
2. Historical reconstruction: Systematic reconstruction of historical auroral records from diverse cultural sources (Lee & Liu, 2023; Maraschi, 2018)
3. Cultural analysis: Attention to cultural, religious, and political contexts mediating auroral interpretation (Brekke & Egeland, 1983; Goshu & Ridwan, 2024a)
4. Synthetic integration: Integration of physical, historical, and cultural knowledge into a unified framework

Table 6. Research Agenda for Astromythology: The "Plasma-Portent" Model

Research Domain	Key Questions	Methodological Approaches
Physical Calibration	How can historical auroral descriptions be calibrated against physical storm intensity?	Spectral analysis; Kp/Dst reconstruction; IBC classification
Historical Reconstruction	What is the full spatial and temporal extent of historical auroral records?	Archival research; dendrochronology (^{14}C, ^{10}Be); oral history
Cultural Analysis	How do cultural, religious, and political contexts mediate auroral interpretation?	Comparative religion; ethnohistory; discourse analysis
Synthetic Integration	How do the magnetosphere and mythosphere interact as coupled systems?	Transdisciplinary modeling; digital humanities; GIS mapping

Table 6 presents a strategic roadmap for the emerging interdisciplinary field of astromythology, operationalizing the "plasma-portent" model's research agenda across four interconnected domains. Physical Calibration addresses the methodological challenge of correlating historical auroral descriptions with storm intensity through spectral analysis and Kp/Dst reconstruction (Rees & Luckey, 1974). Historical Reconstruction extends the space weather record via archival research and dendrochronology (^{14}C, ^{10}Be), leveraging Chinese official histories spanning 511–1876 CE and European chronicles (Lee & Liu, 2023; Maraschi, 2018). Cultural Analysis employs comparative religion and ethnohistory to examine how cultural contexts mediate auroral interpretation, as demonstrated by the cross-cultural "blood/war" association (Brekke & Egeland, 1983). Synthetic Integration proposes transdisciplinary modeling and GIS mapping to investigate magnetosphere-mythosphere coupling (Hwang et al., 2023;

Eliot, 1997). This framework provides a rigorous methodological foundation for integrating physical and cultural knowledge systems.

V. Conclusion

The aurora borealis stands as humanity's oldest continuous laboratory, a physical phenomenon that forces us to reconcile cosmic brutality with transcendent meaning-making. This paper has demonstrated that the aurora is not merely a spectacle to be observed but a phenomenon to be interpreted, a "plasma-portent" bridging the magnetosphere and mythosphere.

We have established that geomagnetic forcing systematically influences cultural output. The Trigger Threshold Hypothesis ($Kp \geq 7$) identifies the physical condition for portentous events. Chromatic Theology demonstrates that red aurorae consistently evoke "blood/war" omens across unrelated cultures. The mythosphere functions as a cultural magnetometer for reconstructing historical space weather.

The synthesis validates the Intensity Hypothesis: geomagnetic forcing directly scales with the intensity of cultural and religious responses. The 774–775 CE Miyake events exemplify the power of this integrative approach.

The aurora thus emerges as a unique phenomenon illuminating both the upper atmosphere and the depths of human meaning-making. The proposed field of astromythology offers a roadmap for continuing this dialogue, integrating solar physics, historical climatology, and comparative religion into a unified framework for understanding the relationship between humanity and the cosmos.

References

Borwein, N. S. (2025). Ways of theorizing and transient phenomena (Section I). In N. S.

Brekke, A., & Egeland, A. (1983). The northern light: From mythology to space research. Springer-Verlag. https://doi.org/10.1007/978-3-642-81885-5

Broome, J. D., Cook, D., & Davíðsdóttir, B. (2024). Heavenly lights: An exploratory review of auroral ecosystem services and disservices. Ecosystem Services, 67, Article 101626. https://doi.org/10.1016/j.ecoser.2024.101626

Dungey, J. W. (1961). Interplanetary magnetic field and the auroral zones. Physical Review Letters, 6(2), 47–48. https://doi.org/10.1103/PhysRevLett.6.47

Eather, R. H., & Mende, S. B. (1971). Airborne observations of auroral precipitation patterns. Journal of Geophysical Research, 76(7), 1746–1755. https://doi.org/10.1029/JA076i007p01746

Echim, M. M., Maggiolo, R., Roth, M., & De Keyser, J. (2009). A magnetospheric generator driving ion and electron acceleration and electric currents in a discrete auroral arc observed by Cluster and DMSP. Geophysical Research Letters, 36(22), L22106. https://doi.org/10.1029/2009GL038343

Eliot, A. (1997). The timeless myths: How ancient legends influence the modern world. Truman Talley/Meridian.

Falck Ytter, H. (1999). Aurora: The northern lights in mythology, history and science (R. Alexander, Trans.). Bell Pond Books.

Goshu, B.S. and M. Ridwa, (2024), Celestial connections: Exploring the intersection of astronomy and the Ethiopian biblical canon, SIASAT, 9 (4), 249-264

Goshu, B.S. and M. Ridwan, (2024a), Auroras: A Harmonious Blend of Natural Science and Human Culture, Lakhomi Journal Scientific Journal of Culture, 5 (3), 151-164

Goshu, B.S., (2024), Mapping solar variability of equatorial sunspots and plasma flows, Brazilian Journal of Science, 3 (9), 49-64

Goshu, B.S., (2024a), Understanding the Influence of Geomagnetic Storms on Earth's Atmospheric Dynamics in April 2022 And 2023, Budapest International Research in Exact Sciences (BirEx) Journal, 6 (4), 282-298

Hayakawa, H., Ebihara, Y., & Willis, D. M. (2018). Low-latitude aurorae during the extreme space weather events in 1859. The Astrophysical Journal, 868(2), Article 110. https://doi.org/10.3847/1538-4357/aae47c

Hayakawa, H., Ebihara, Y., Willis, D. M., Toriumi, S., Iju, T., Hattori, K., Wild, M. N., Oliveira, D. M., Ermolli, I., Ribeiro, J. R., Correia, A. P., & Soma, M. (2019). Temporal and spatial evolutions of a large sunspot group and great auroral storms around the Carrington event in 1859. The Astrophysical Journal, 885(1), Article 9. https://doi.org/10.3847/1538-4357/ab3a2e

Holzworth, R. H. (1975). Folklore and the aurora. Eos, Transactions American Geophysical Union, 56(10), 686–688. https://doi.org/10.1029/EO056i010p00686

Hwang, K.-J., Nakamura, R., Eastwood, J. P., & Fuselier, S. A. (2023). Cross-scale processes of magnetic reconnection. Space Science Reviews, 219(8), Article 70. https://doi.org/10.1007/s11214-023-01010-9

Janhunen, P. (2004). Different Alfvén wave acceleration processes of electrons in the auroral current region. Annales Geophysicae, 22(4), 1373–1382. https://doi.org/10.5194/angeo-22-1373-2004

Jones, D. W. (2007). The game. Firebird.

Judge, D. L. (1972). The production of auroral 6300 Å emission by low-energy electrons. Journal of Geophysical Research, 77(7), 1220–1226. https://doi.org/10.1029/JA077i007p01220

Kivelson, M. G., & Russell, C. T. (Eds.). (1995). Introduction to space physics. Cambridge University Press. https://doi.org/10.1017/9781139878296

Lee, P.-H., & Liu, J.-Y. (2023). Response of aurora candidates in the Chinese official histories to the space climate during 511–1876. Earth, Planets and Space, *75*, Article 138. https://doi.org/10.1186/s40623-023-01889-4

Love, J. J., Rigler, E. J., & Pulkkinen, A. (2019). Intensity and impact of the New York Railroad superstorm of May 1921. Space Weather, 17(7), 1018–1037. https://doi.org/10.1029/2019SW002190

Lysak, R. L. (2023). Kinetic Alfvén waves and auroral particle acceleration: A review. Space Science Reviews, 219(6), Article 45. https://doi.org/10.1007/s11214-023-00991-x

Maraschi, A. (2018). Red lights in the sky, hunger in sight: Aurora borealis and famine between experience and rhetoric in the early Middle Ages. Revista de História da Sociedade e da Cultura, 18, 301–322. https://doi.org/10.14195/1645-2259_18_16

Mashhood, H. (2025). Aurora Borealis: Scientific mechanisms, geomagnetic influences, and cultural significance. Social Science Academic, 3(1), 77–84. https://doi.org/10.37680/ssa.v3i1.8195

Miyake, F., Nagaya, K., Masuda, K., & Nakamura, T. (2012). A signature of cosmic-ray increase in AD 774–775 from tree rings in Japan. Nature, 486(7402), 240–242. https://doi.org/10.1038/nature11123

Moreno Cárdenas, F., Cristancho Sánchez, S., & Vargas Domínguez, S. (2016). The grand aurorae borealis seen in Colombia in 1859. Advances in Space Research, 57(1), 257–267. https://doi.org/10.1016/j.asr.2015.08.026

Novitsky, T., & Lee, A. S. (2023). Spirits dancing: The night sky, indigenous knowledge, and living connections to the cosmos. Minnesota Historical Society Press.

Odenwald, S. (2015). Solar storms: 2000 years of human calamity. CreateSpace.
Public behaviour during severe space weather events. (n.d.). Lancaster University. https://eprints.lancs.ac.uk
Rees, M. H., & Luckey, D. (1974). Auroral electron energy derived from ratio of spectroscopic emissions 1. Model computations. Journal of Geophysical Research, 79(34), 5181–5186. https://doi.org/10.1029/JA079i034p05181
Sadeghi, S., Emami, M. R., & Sadeghi, S. (2019). Large-scale altitude distribution profile of auroral parallel electric potentials: A statistical analysis of Cluster data. Advances in Space Research, 63(12), 4009–4020. https://doi.org/10.1016/j.asr.2019.03.018
Schroeder, J. W. R., Howes, G. G., Kletzing, C. A., Skiff, F., Carter, T. A., Vincena, S., & Dorfman, S. (2021). Laboratory measurements of the physics of auroral electron acceleration by Alfvén waves. Nature Communications, 12, 3103. https://doi.org/10.1038/s41467-021-23377-5
Siscoe, G. L. (1978). An historical footnote on the origin of "Aurora Borealis." Eos, Transactions American Geophysical Union, 59(12), 994–997. https://doi.org/10.1029/EO059i012p00994
Tian, S., Yao, Z., Wygant, J. R., Lysak, R. L., Bortnik, J., Lyons, L. R., & Liang, J. (2026). Evidence for Alfvén waves powering auroral arc via a static electric potential drop. Nature Communications, 17, 297. https://doi.org/10.1038/s41467-026-70013-9
Usoskin, I. G., Kovaltsov, G. A., & Mironova, I. A. (2019). The celestial sign in the Anglo-Saxon Chronicle in the 770s: Insights on contemporary solar activity. Solar Physics, 294(4), Article 48. https://doi.org/10.1007/s11207-019-1439-6
Usoskin, I. G., Kromer, B., Ludlow, F., Beer, J., Friedrich, M., Kovaltsov, G. A., Solanki, S. K., & Wacker, L. (2013). The AD775 cosmic event revisited: The Sun is to blame. Astronomy & Astrophysics, 552, L3. https://doi.org/10.1051/0004-6361/201321080
Walsh, B. M., Chappell, C. R., & Denton, R. E. (2013). The role of magnetospheric plasma in solar wind-magnetosphere coupling: A review. Journal of Atmospheric and Solar-Terrestrial Physics, 85-86, 1–14. https://doi.org/10.1016/j.jastp.2021.105687
Watt, C. E. J., & Rankin, R. (2008). Electron trapping in shear Alfvén waves that power the aurora. Physical Review Letters, 100(3), 035003. https://doi.org/10.1103/PhysRevLett.100.035003
Wild, J. (2006). Look out, aurorae about! Astronomy & Geophysics, 47(1), 1.11–1.13. https://doi.org/10.1111/j.1468-4004.2006.47111.x